

Assembly of Helical Structures in Systems with Competing Interactions under Cylindrical Confinement

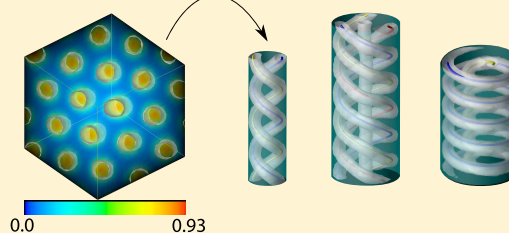
Horacio Serna,[†] Eva G. Noya,[‡] and W. T. Gózdź^{*,†}

[†]Institute of Physical Chemistry of the Polish Academy of Sciences, Kasprzaka 44/52, 01-224 Warsaw, Poland

[‡]Instituto de Química Física Rocasolano, Consejo Superior de Investigaciones Científicas (CSIC), Calle Serrano 119, 28006 Madrid, Spain

ABSTRACT: The behavior under confinement of nanoparticles interacting with the short-range attraction and long-range repulsion potential is studied by means of Monte Carlo simulations in the grand canonical ensemble. The study is performed at thermodynamic conditions at which a hexagonal cylindrical phase is the most stable phase in bulk. In these conditions, cylindrical confinement promotes the formation of helical structures whose morphology depends upon both the pore radius and boundary conditions. As the pore radius increases, the fluid undergoes a series of structural transitions going from single to multiple intertwined helices to concentric helical structures. When the pore ends are closed by planar walls, ring and toroidal clusters are formed next to these walls. Dependent upon the cylinder length, molecules away from the pore edges can either keep growing into ring and toroidal aggregates or arrange into helical structures. It is demonstrated that the system behaves in cylindrical confinement in the same way as the block copolymer systems. Such behavior has not been observed for the colloidal systems in cylindrical confinement with only repulsive interactions.

Self-assembled colloidal aggregates in bulk and confined in a cylinder



INTRODUCTION

Systems with competing interactions are widespread in nature. Mixtures of surfactants, lipids, diblock copolymers, and colloids are examples of such systems. They are important in biology and industry. It has been demonstrated that all of these systems behave in a similar way, despite the different molecular compositions of their constituents.^{1–3} Lamellar, hexagonal, and triply periodic phases, such as gyroid or diamond structures, are found in all of these systems, which exhibit phase diagrams with the same topology. As a result of its relevance in technological applications, among these systems, diblock polymers have been more intensively studied, both experimentally and theoretically. Lipid mixtures have also attracted much attention as a result of their role as basic building blocks in living organisms. In colloids, competing interactions have been traditionally assumed to be attainable by combining short-range attractive depletion with long-range repulsive electrostatic interactions. However, this view is starting to be questioned,⁴ because despite the tunability of these interactions in colloids, the formation of mesophases in bulk predicted by theory and simulations remains elusive in experiments. The remarkable similarity between the bulk phase diagram of simple isotropic short-range attraction and long-range repulsion (SALR) models and that of diblock copolymers has been confirmed by recent computer simulations.⁵ In this paper, we show that this similarity also extends to confined systems. With this aim, we performed computer simulations for a three-dimensional off-lattice model for which the phase diagram has been recently calculated by

molecular simulations.⁵ We found that the behavior of the hexagonal phase in cylindrical pores is very similar for polymeric and colloidal systems characterized by competing interactions. We may expect that many results obtained thus far for polymers^{6,7} might be also applicable to colloidal systems. Thus, the knowledge already obtained for polymers can be used as a guidance and inspiration for studies of colloidal systems with competing interactions.

We stress that the structures in the system studied here are substantially different from previously studied helical structures of colloidal particles in cylindrical confinement. Previously studied systems were composed of particles interacting with hard or soft repulsive potential, such as hard spheres⁸ or Yukawa⁹ potentials, and the helices were observed at a high pressure and for very narrow cylinders of the order of a few hard core diameters. Our colloidal system is unique in the sense that its behavior is like the behavior of block copolymers. We observe the helical structure for not only narrow cylinders but also wide cylinders and at a low pressure. The structures that we obtain are almost identical to the structures observed in block copolymers, despite different molecular compositions of these systems. We show that the colloidal systems with competing interactions may behave in a way similar to block copolymer systems in not only bulk but also confined geometry. The formation of helical structures in cylindrical

Received: October 7, 2018

Revised: December 3, 2018

Published: December 27, 2018

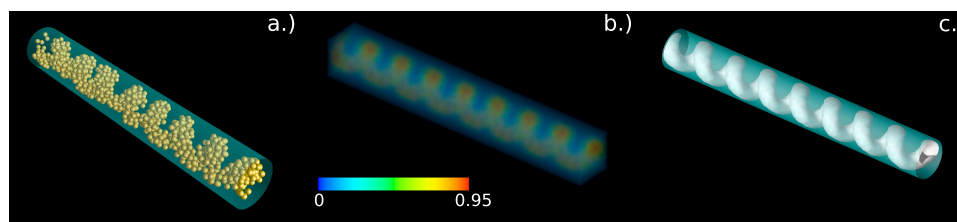


Figure 1. Illustration of the structure of the simulated fluid. (a) Snapshot showing the locations of the molecules. (b) Average local density, where the color denotes the values of the local density according to the color map below the image. (c) Isosurface obtained for the value of the local density $\rho_{\text{iso}} = 0.4$. The radius of the confining cylinder is $R = 3.5\sigma$, and its length is $L = 60\sigma$. The mean density is $\langle \rho \rangle = 0.279$.

confinement is quite common and present in many different systems.^{10,11} However, the fact that such different systems as colloidal particles and block copolymers show striking similarity in a number of helical structures is unusual and presented for the first time in our work. Experimentally, colloidal crystals with a helix-like shape have been obtained under cylindrical confinement.^{12–14} These helical structures co-assemble with very narrow pores (just few colloidal particle diameters), where colloidal particles behave like hard spheres. Similar findings were obtained numerically.⁸ The structures that we present here are different from those found before for colloidal spheres because the system that we simulate has competing interactions and does not need a very tight confinement to self-assemble into helices, as we show in our results. Recently, an experimental protocol that allows for the control of the morphology in block copolymer nanorods confined into nanopores was developed.¹⁵ The multi-helical structures obtained in that investigation are quite similar to our findings.

MODEL AND SIMULATION METHOD

In complex fluids, such as colloidal suspensions, the short-range attraction comes from entropic depletion forces and the long-range repulsion is due to electrostatic interactions.¹⁶ Regardless of the mathematical shape of the SALR potential, there exists universality in not only the ordered phases that appear in each case but also the sequence of appearance: crystal-cluster phase, cylindrical phase, double gyroid phase, and lamellar phase. This has been demonstrated by theory and simulations.^{1,2,5,17} In this paper, interactions between the molecules are described by the square-well-linear potential given by

$$u_{\text{SALR}}(r) = \begin{cases} \infty & r < \sigma \\ -\varepsilon & \sigma < r < \lambda\sigma \\ \zeta\varepsilon(\kappa - r/\sigma) & \lambda\sigma < r < \kappa\sigma \\ 0 & r > \kappa\sigma \end{cases} \quad (1)$$

The unit of energy is ε , and the unit of distance is σ , where σ is the hard core diameter. ε and σ are used to express the temperature, chemical potential, internal energy, density, and distance in reduced units. We set the values $\zeta = 0.05$, $\lambda = 1.5$, and $\kappa = 4$ as those in the simulations of the bulk system.⁵

The Monte Carlo simulations were performed in the grand canonical ensemble at fixed chemical potential, temperature, and volume (μ , V , and T). The simulated systems contained between 300 and 3300 particles. Systems were equilibrated over $1\text{--}15 \times 10^9$ Monte Carlo steps depending upon the system size. Averages were taken over 5×10^8 Monte Carlo steps. A Monte Carlo step consisted of a trial move that can be a displacement, addition, or deletion of a molecule.

In this work, we focused on the study of the behavior of the SALR fluid confined in a hard repulsive cylinder. Both axially periodic and finite pores whose edges are closed by hard walls were considered. The effects of the cylinder radius (R) and length (L) were investigated by performing simulations of pores with varying radius $2\sigma < R < 14\sigma$

and length $15\sigma < L < 60\sigma$. The radius R is defined here as the distance from the center of the cylinder to the point where the external potential is infinite. The study was conducted at a thermodynamic state at which the hexagonal cylindrical phase is the most stable phase in bulk. The chemical potential of the bulk hexagonal phase at a given temperature and density was estimated from a series of simulations at different chemical potentials at the corresponding temperature. In particular, we chose a state at $T = 0.35$ and $\mu = -2.1$, which is located roughly at the center of the stability region of the hexagonal phase according to the phase diagram reported in ref 5. We checked that the structure of the fluid at these conditions indeed coincides with that of the hexagonal cylindrical phase.

Examples of the simulation results are presented in Figure 1. A snapshot of a typical configuration of the confined fluid is presented in Figure 1a. Figure 1b shows the local density, where colors indicate the value of the local density according to the color map located below the image. Because it may be difficult to see the structure of the fluid from the three-dimensional local density images, the isosurface obtained for a fixed value of the local density is also given. An example of such an isosurface is presented in Figure 1c. The value of the density used to plot the isosurface is $\rho_{\text{iso}} = 0.4$.

RESULTS

Let us start by presenting the results for the fluid confined in an axially periodic cylinder (i.e., applying periodic boundary conditions along the cylinder axial direction). The summary of the results of our calculations is presented in Figure 2. It is interesting to note that the molecules forming the helical structures are arranged along curves, which can be described by an equation of a helix, $x(t) = a \cos(t)$, $y(t) = a \sin(t)$, $z(t) = bt$, where $t \in (0, 2\pi)$ is the independent variable, a is the radius, and $2\pi b$ describes the vertical separation of the loops of the helix. These curves are shown in Figure 2 with different colors (red, green, blue, and yellow).

At the chosen thermodynamic state, the molecules self-assemble in straight cylinders that are arranged in a hexagonal lattice in bulk.^{1,18} According to our calculations, the cylindrical confinement destroys this order, at least for pores with a radius within the range of $3.5\sigma < R < 14\sigma$. When the radius of the confining cylinder is comparable to the equilibrium radius of the cylindrical aggregates in the bulk hexagonal phase ($R \approx 2\sigma$), molecules still form a straight tubular structure. In this case, the geometrical restrictions are incompatible with any non-straight arrangement. However, when the pore diameter reaches the value of the order of the equilibrium distance between neighbor cylinders in the bulk hexagonal phase ($2R > 6\sigma$), there is a structural transition to helical arrangements. Above this threshold, the system organizes into single or multiple helical structures, initially formed by one layer that is transformed into concentric multi-layer helical structures when the pore radius increases. The growth of an additional layer always starts by the formation of a straight cylinder at the center of the previously formed helical structure. This straight

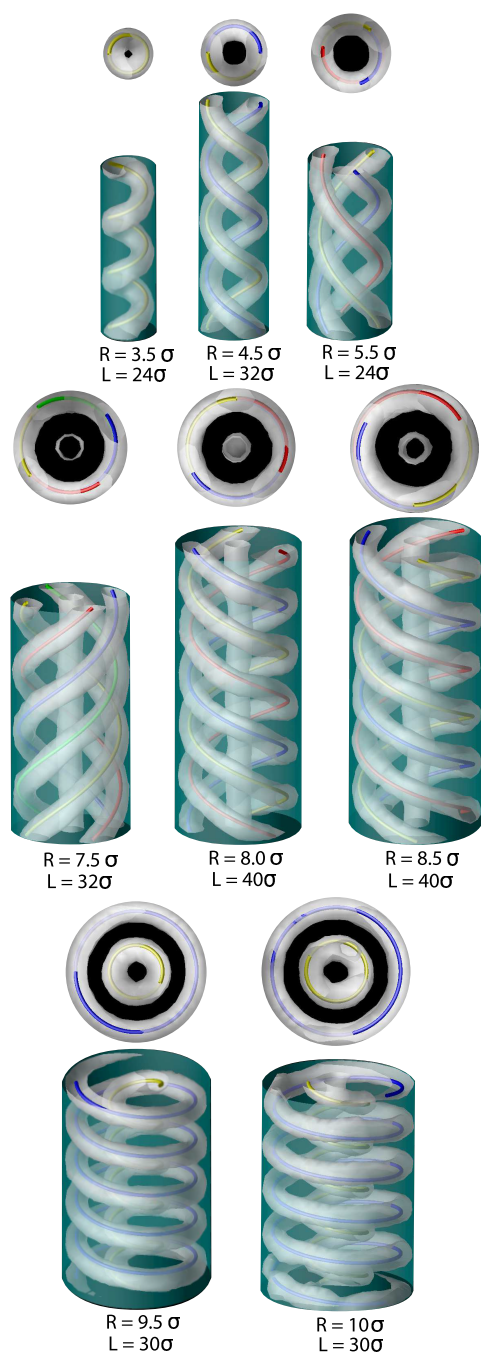


Figure 2. Possible configurations of the hexagonal phase in cylindrical confinement for different values of the cylinder radius $3.5\sigma \leq R \leq 10\sigma$ for axially periodic pores. The gray surface shows points with local density $\rho_{\text{iso}} = 0.4$. Two different views of each configuration are depicted: along the parallel (bottom images) and perpendicular (top images) directions to the cylinder axis. The length of the confining cylinder is $24\sigma \leq L \leq 40\sigma$.

cylindrical aggregate is able to survive over a relatively broad range of radii (now lower than the cylinder equilibrium distance in bulk, probably as a result of the softness of the more external coaxial helical structure), until, at a given radius size, a transformation into a second helical structure concentric to the external helix becomes favorable. Interestingly, these structures are remarkably similar to those obtained for confined surfactants¹⁹ and diblock copolymers.⁷ The behavior of all of these systems is determined by competing interactions,

although the physical origin is different in each case. In block copolymers, interactions are anisotropic and emerge from the immiscibility of different polymer components. Here, we have considered the simplest case of confining potential (hard cylinder), but it seems reasonable that the main trends will not change when softer confining potentials are used. This idea is also supported by the similarity between our simulations and the real experiments in block copolymers. As already mentioned, it is known that the systems with competing interactions have phase diagrams with the same topology in bulk. Our results strongly support the idea that this universality also extends to the behavior under confinement. This is also supported by the recent theoretical calculations that show that the gyroid phase under confinement and under shear exhibit a very similar behavior in both systems.²⁰

We have analyzed the effect of boundary conditions on the structure of the fluid for two representative values of the cylinder radius. For a narrow pore with a diameter close to the distance between neighbor cylinders in the bulk phase, we have observed the formation of a single helix, as presented in Figure 4a. We have investigated the effect of the length in axially periodic pores. Note that the length of the system can have a strong impact on the structure of the helical arrangements, depending upon whether the chosen system is commensurate or not with the equilibrium pitch of the helix in the thermodynamic limit. We have observed that the helical structure is maintained for all considered lengths up to $L = 60\sigma$. However, the helical structure behaves like an elastic spring that can be stretched or shortened with an energy penalty but without rupturing it when the system length is varied. Of course, the helix cannot be stretched to a straight line. At some length, it becomes unstable and a new structure is formed with increased numbers of coils in the helix. The equilibrium period of the helix can be obtained by performing simulations at different lengths. In Figure 3, we present the values of the energy and density calculated for different values of the cylinder length. Only the points with the lowest energy for a given number of pitches in the cylinder are shown. We observe that the distance between minima, for the single and double helix, is between 7.5σ and 8σ . We estimate that the periodicity of the single helix is of the order of $L_p \approx 7.5\sigma$ and the periodicity of the double helix is of the order of $L_p \approx 16\sigma$. The size and shape of the confining walls determine the topology of the structures under confinement. It has to be noted that, in the case of cylinders, the colloidal particles form helices for almost all of the values of the cylinder radius, unless the cylinder is very narrow. To avoid formation of helical structures, the cross section of the confining cylinder must be changed to a triangle, a square, or a hexagon.

We have also considered the case of a finite cylinder whose edges are closed by hard planar surfaces. The external potential is infinite at $z = 0$ and L , where z is the distance along the axis of the cylinder. In this case, disk-like clusters are formed at both ends of the confined cylinder. Molecules in the middle of the cylinder can arrange in two different ways depending upon the pore length. At some system lengths, molecules assemble into disk-like clusters along all of the cylinder, whereas in other cases, a single helical cluster forms at the central region of the pore capped with two disk-like clusters at the cylinder ends. Interestingly, structures composed of only disk-like clusters exist, even for very long pores. We speculate that these structures appear when the pore length does not match the preferred pitch of a helix.

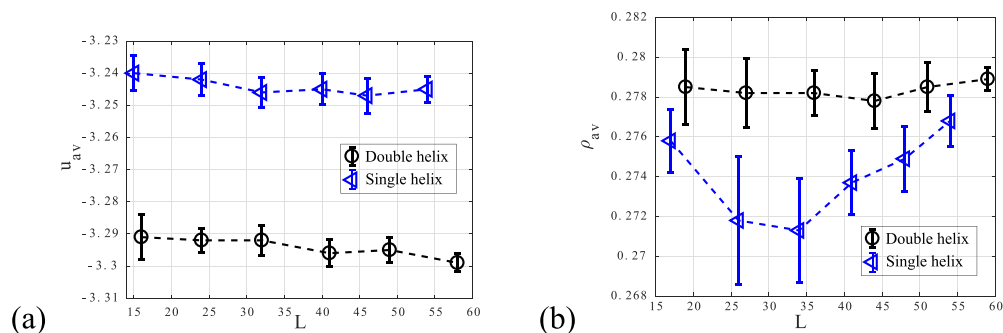


Figure 3. (a) Average energy per particle and (b) average number density as a function of the cylinder length for the configurations with a single and double helix. The radii of the cylindrical pores are $R = 3.5\sigma$ for a single helix and $R = 4.5\sigma$ for two helices.

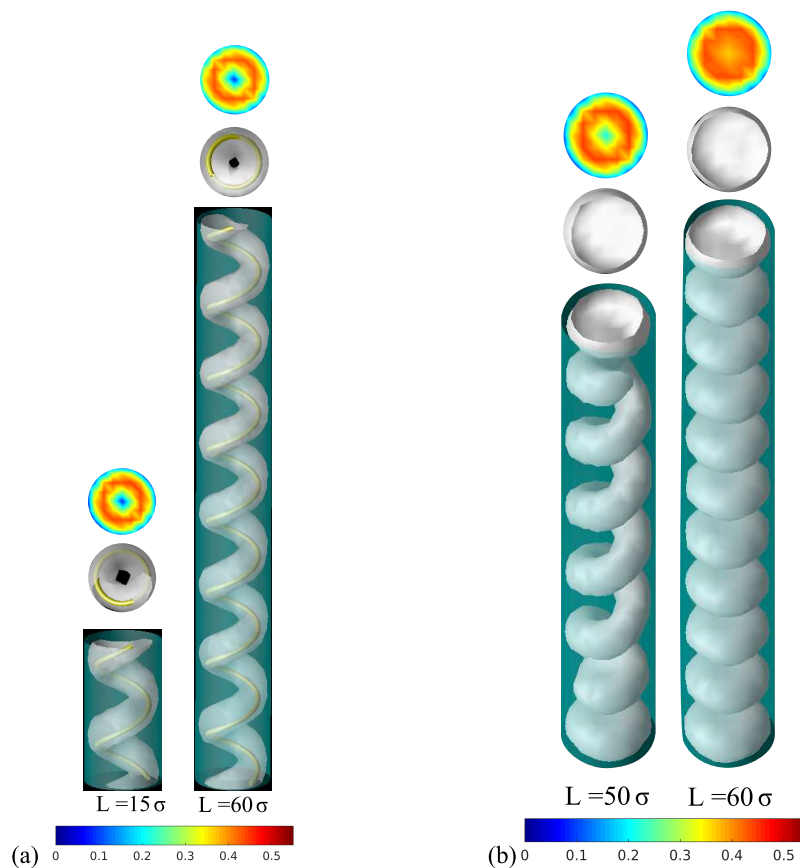


Figure 4. Single helices formed in cylindrical pores of radius $R = 3.5\sigma$. The configurations were obtained for (a) axially periodic pores and (b) pores with closed ends. The gray surface shows points with local density $\rho_{iso} = 0.4$. The top view of each image displays the local density projected on a plane perpendicular to the cylinder axis. The local density is represented by colors according to the color map below the image. The mean densities are (a) for shorter cylinder $\langle\rho\rangle = 0.284$ and longer cylinder $\langle\rho\rangle = 0.279$ and (b) for shorter cylinder $\langle\rho\rangle = 0.3288$ and longer cylinder $\langle\rho\rangle = 0.286$.

The second case corresponds to a larger radius of the cylinder for which two intertwined helices are formed. Simulations of axially periodic pores of varying lengths again reveal that the helical structure is always formed, irrespective of the system length. Our simulations indicate that the period of this double helical structure is larger than that of the single helix, of the order of $L_p \approx 16\sigma$, i.e., roughly twice that of the single helix. The smallest periodic element is shown in Figure 5a on the left side. For the closed pores, we have observed that the particles self-assemble into toroidal clusters at both ends of the pore. Analogously to the case of the narrower pore described above, particles at the central part of the pore can adopt two different configurations depending upon the pore

length, one configuration consisting solely of toroidal clusters through the whole pore and another configuration in which molecules at the pore center self-assemble into a double helix that is connected to the toroidal clusters at the pore edges (see Figure 5b).

It should be noted that the helices formed in our simulations were either right- or left-handed, without any preference for either one. We have not found any differences in their energy or stability because they are like mirror images of each other. An example of two helical structures that are like mirror images is presented in Figure 6. Obviously, in double helical structures, the two intertwined helices always exhibit the same handedness, which can be explained by considering the

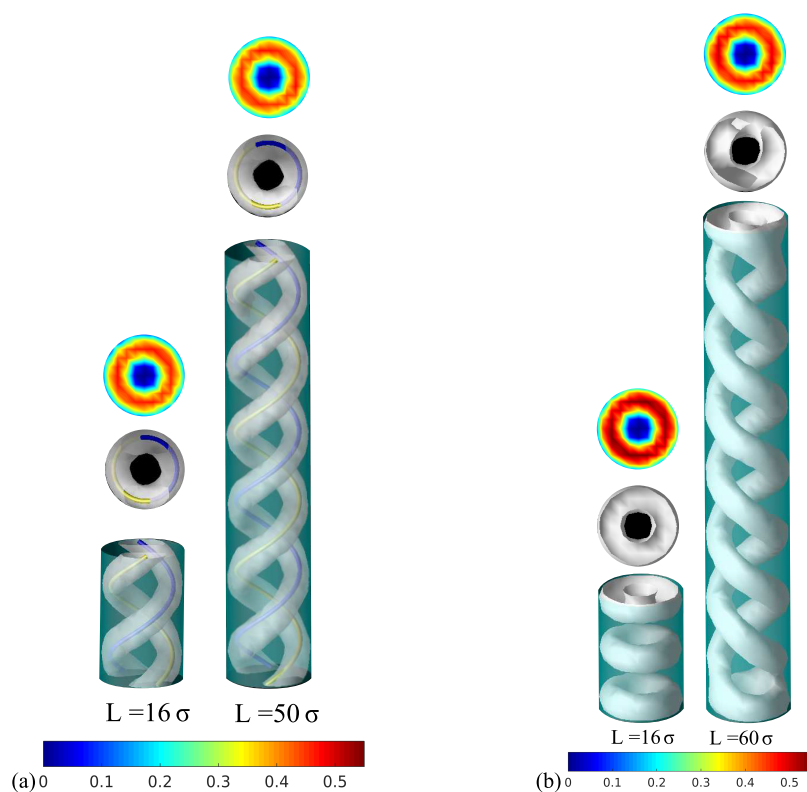


Figure 5. Double helices formed in cylindrical pores of radius $R = 4.5\sigma$. The configurations were obtained for (a) axially periodic pores and (b) pores with closed ends. The gray surface shows points with local density $\rho = 0.4$. The top view of each image shows the local density projected on a plane perpendicular to the cylinder axis. The local density is represented by colors according to the color map below the image. The mean densities are (a) for shorter cylinder $\langle \rho \rangle = 0.283$ and longer cylinder $\langle \rho \rangle = 0.280$ and (b) for shorter cylinder $\langle \rho \rangle = 0.329$ and longer cylinder $\langle \rho \rangle = 0.295$.

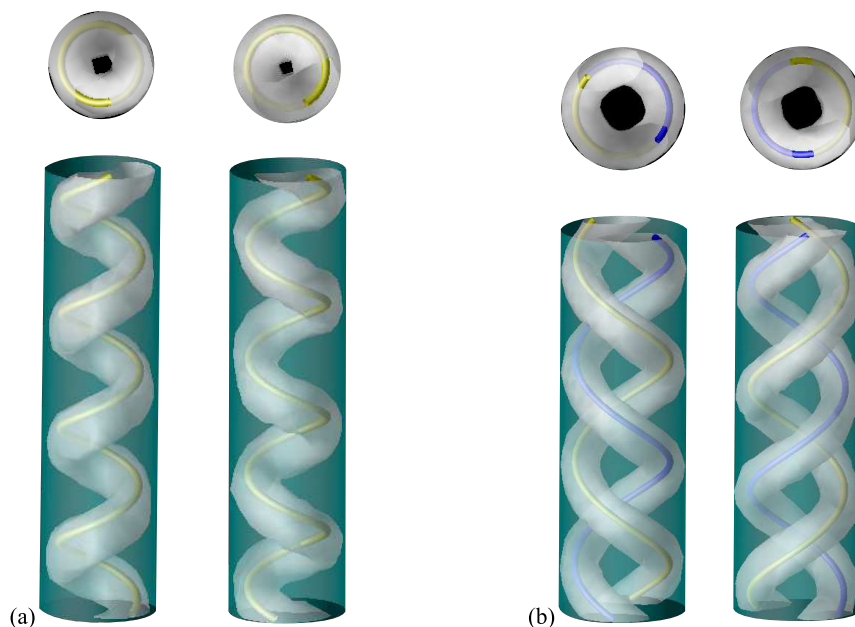


Figure 6. Left- and right-handed configurations obtained for the same set of parameters of the confining pore: (a) single helix at $R = 3.5\sigma$, $L = 30\sigma$, and $\langle \rho \rangle = 0.282$ and (b) double helix at $R = 4.5\sigma$, $L = 30\sigma$, and $\langle \rho \rangle = 0.280$.

packing and topological properties of helices. This also holds for concentric helical structures. The handedness of the inner and outer helices was always the same. Another interesting fact is that, for large pores, it is common that the confined fluid can assemble into more than one stable structure for a given set of pore parameters. An example of two configurations existing for

the same pore dimensions is presented in Figure 7. The particles can self-assemble in either a double or triple helix. These structures exhibit 2- and 3-fold rotational symmetry along the pore axial direction, respectively; i.e., the double helix structure superimposes into itself when a rotation of $n\pi$ radians about the pore axis is performed, and the same is true for the

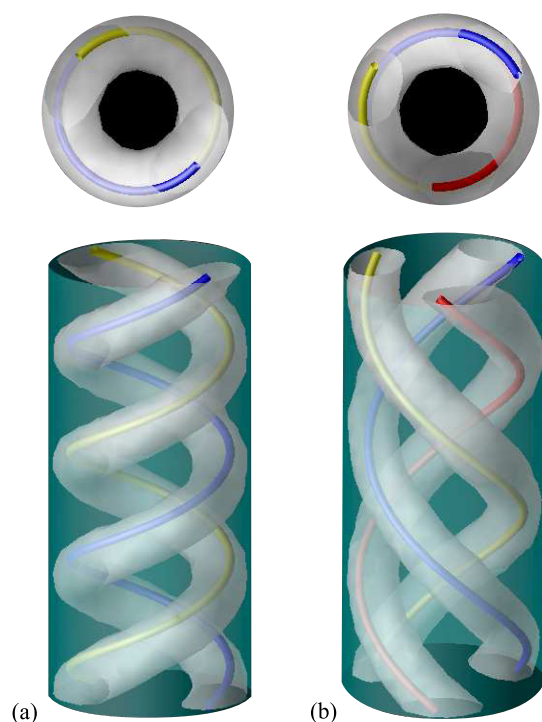


Figure 7. Example of two different configurations obtained for the same set of parameters of the confining pore at $R = 5.5\sigma$ and $L = 26\sigma$: (a) $\langle\rho\rangle = 0.268$ for two helices and (b) $\langle\rho\rangle = 0.265$ for three helices.

triple helical structure for rotation angles of $n2\pi/3$ radians, with n being an integer number. The existence of two types of structures is rather common and occurs over quite a broad range of radii for not only the helical structures consisting of a single shell but also the structures composed of concentric helices that appear for wider pores. We can speculate that, in the systems we have studied and in general in SALR systems, one may observe two or more structures with the same free energy, but to check this hypothesis, extensive calculations of the free energy for different radii and lengths of the confining cylinder are required.

SUMMARY AND CONCLUSION

We have demonstrated how the structure of the hexagonal phase formed in the fluid interacting with SALR potential is modified by confinement. We have observed that cylindrical confinement induces the formation of helical structures over the whole range of pore radii considered in this work. The pitch and radius of the helical structures can be tuned by adjusting the width of the confining cylinder. For wider cylinders, the confined fluid organizes into intertwined or concentrically arranged helices. In all of the structures formed by more than one helix, all helices exhibited the same handedness. Looking at the density profiles of concentric helical structures along the pore axial direction, one can see patterns formed by concentric rings of high density intercalated with rings of low density. The distance between these concentric rings remains constant and depends upon the range of repulsive and attractive interactions of the interatomic potential.

We may expect that the formation of helical structures can also be realized in any system characterized by competing interactions when confined in a cylindrical pore. In most such systems, the hexagonal phase is stable. Examples of such

systems are mixtures containing surfactants, lipids in water, or block copolymers. They are widespread in nature and industry. We hope that our investigations may help to understand the formation of similar structures in living organisms and designing technological processes for the development of new materials. Recent simulational studies have shown that one potential difficulty in observing mesophases in colloidal experiments (provided that the experimental problems in obtaining a colloidal system with an isotropic SALR interaction can be solved⁴) is trapping the system in a variety of metastable states.²¹ We can speculate that the investigation of ordered structures in simple confined geometries may be much easier than in bulk because the number of possible metastable states is likely to be reduced in tight confinement conditions. We hope that the results of computer simulations presented here may be used as a guidance for new experimental studies of colloidal systems with competing interactions.

AUTHOR INFORMATION

Corresponding Author

*E-mail: wtg@ichf.edu.pl

ORCID

W. T. Gózdź: [0000-0003-4506-6831](https://orcid.org/0000-0003-4506-6831)

Notes

The authors declare no competing financial interest.

ACKNOWLEDGMENTS

The authors thank A. Ciach and A. Meira for helpful discussion and support of our work. This publication is part of a project that has received funding from the European Union's Horizon 2020 research and innovation programme under the Marie Skłodowska-Curie Grant Agreement 711859 to Horacio Serna and 734276 to Horacio Serna and W. T. Gózdź. Additional funding was received from the Ministry of Science and Higher Education of Poland for the Project 734276 in the years 2017–2018 (Agreement 3854/H2020/17/2018/2) and the implementation of the International Co-financed Project 711859 in the years 2017–2021. The authors acknowledge the support from NCN, Grant 2015/19/B/ST3/03122, and the Agencia Estatal de Investigación and the Fondo Europeo de Desarrollo Regional (FEDER), Grant FIS2017-89361-C3-2-P.

REFERENCES

- (1) Ciach, A.; Gózdź, W. Mesoscopic description of network-forming clusters of weakly charged colloids. *Condens. Matter Phys.* **2010**, *13*, 1–12.
- (2) Ciach, A.; Pekalski, J.; Gózdź, W. Origin of similarity of phase diagrams in amphiphilic and colloidal systems with competing interactions. *Soft Matter* **2013**, *9*, 6301–6308.
- (3) Edelman, M.; Roth, R. Gyroid phase of fluids with spherically symmetric competing interactions. *Phys. Rev. E: Stat. Phys., Plasmas, Fluids, Relat. Interdiscip. Top.* **2016**, *93*, 062146.
- (4) Royall, C. P. Hunting mermaids in real space: Known knowns, known unknowns and unknown unknowns. *Soft Matter* **2018**, *14*, 4020–4028.
- (5) Zhuang, Y.; Zhang, K.; Charbonneau, P. Equilibrium Phase Behavior of a Continuous-Space Microphase Former. *Phys. Rev. Lett.* **2016**, *116*, 098301.
- (6) Dobryjal, P.; Xiang, H.; Kazuyuki, M.; Chen, J.-T.; Jinnai, H.; Russell, T. P. Cylindrically Confined Diblock Copolymers. *Macromolecules* **2009**, *42*, 9082–9088.
- (7) Shi, A.-C.; Li, B. Self-assembly of diblock copolymers under confinement. *Soft Matter* **2013**, *9*, 1398–1413.

- (8) Fu, L.; Bian, C.; Shields, C. W.; Cruz, D. F.; Lopez, G. P.; Charbonneau, P. Assembly of hard spheres in a cylinder: A computational and experimental study. *Soft Matter* **2017**, *13*, 3296–3306.
- (9) Oguz, E. C.; Messina, R.; Loewen, H. Helicity in cylindrically confined Yukawa systems. *EPL (Europhysics Letters)* **2011**, *94*, 28005.
- (10) Bai, J.; Wang, J.; Zeng, X. C. Multiwalled ice helices and ice nanotubes. *Proc. Natl. Acad. Sci. U. S. A.* **2006**, *103*, 19664–19667.
- (11) Wood, D. A.; Santangelo, C. D.; Dinsmore, A. D. Self-assembly on a cylinder: A model system for understanding the constraint of commensurability. *Soft Matter* **2013**, *9*, 10016–10024.
- (12) Li, F.; Badel, X.; Linnros, J.; Wiley, J. B. Fabrication of Colloidal Crystals with Tubular-like Packings. *J. Am. Chem. Soc.* **2005**, *127*, 3268–3269.
- (13) Tymczenko, M.; Marsal, L. F.; Trifonov, T.; Rodriguez, I.; Ramiro-Manzano, F.; Pallares, J.; Rodriguez, A.; Alcubilla, R.; Meseguer, F. Colloidal Crystal Wires. *Adv. Mater.* **2008**, *20*, 2315–2318.
- (14) Jiang, L.; de Folter, J. W. J.; Huang, J.; Philipse, A. P.; Kegel, W. K.; Petukhov, A. V. Helical Colloidal Sphere Structures through Thermo-Reversible Co-Assembly with Molecular Microtubes. *Angew. Chem., Int. Ed.* **2013**, *52*, 3364–3368.
- (15) Cheng, M.-H.; Hsu, Y.-C.; Chang, C.-W.; Ko, H.-W.; Chung, P.-Y.; Chen, J.-T. Blending Homopolymers for Controlling the Morphology Transitions of Block Copolymer Nanorods Confined in Cylindrical Nanopores. *ACS Appl. Mater. Interfaces* **2017**, *9*, 21010–21016.
- (16) Stradner, A.; Sedgwick, H.; Cardinaux, F.; Poon, W. C. K.; Egelhaaf, S. U.; Schurtenberger, P. Equilibrium cluster formation in concentrated protein solutions and colloids. *Nature* **2004**, *432*, 492–495.
- (17) Gózdź, W. T.; Holyst, R. Triply periodic surfaces and multiply continuous structures from the Landau model of microemulsions. *Phys. Rev. E: Stat. Phys., Plasmas, Fluids, Relat. Interdiscip. Top.* **1996**, *54*, 5012–5027.
- (18) Zhuang, Y.; Charbonneau, P. Recent Advances in the Theory and Simulation of Model Colloidal Microphase Formers. *J. Phys. Chem. B* **2016**, *120*, 7775–7782.
- (19) Wu, Y.; Cheng, G.; Katsov, K.; Sides, S. W.; Wang, J.; Tang, J.; Fredrickson, G. H.; Moskovits, M.; Stucky, G. D. Composite mesostructures by nano-confinement. *Nat. Mater.* **2004**, *3*, 816–822.
- (20) Stopper, D.; Roth, R. Nonequilibrium phase transitions of sheared colloidal microphases: Results from dynamical density functional theory. *Phys. Rev. E: Stat. Phys., Plasmas, Fluids, Relat. Interdiscip. Top.* **2018**, *97*, 062602.
- (21) Zhang, T. H.; Klok, J.; Hans Tromp, R.; Groenewold, J.; Kegel, W. K. Non-equilibrium cluster states in colloids with competing interactions. *Soft Matter* **2012**, *8*, 667–672.